Optimization and theoretical modeling of polymer microlens arrays fabricated with the hydrophobic effect

Daniel M. Hartmann, Osman Kibar, and Sadik C. Esener

High-performance polymer microlens arrays were fabricated by means of withdrawing substrates of patterned wettability from a monomer solution. The *f*-number ($f^{\#}$) of formed microlenses was controlled by adjustment of monomer viscosity and surface tension, substrate dipping angle and withdrawal speed, the array fill factor, and the number of dip coats used. An optimum withdrawal speed was identified at which $f^{\#}$ was minimized and array uniformity was maximized. At this optimum, arrays of $f/3.48$ microlenses were fabricated with one dip coat with uniformity of better than $\Delta f/f \sim \pm 3.8\%$. Multiple dip coats allowed for production of $f/1.38$ lens arrays and uniformity of better than $\Delta f/f \sim \pm 5.9\%$. Average $f^{\#}$s were reproducible to within 3.5%. A model was developed to describe the fluid-transfer process by which monomer solution assembles on the hydrophilic domains. The model agrees well with experimental trends.

OCIS codes: 220.3620, 160.5470, 220.4000.

1. Introduction

In today's world of information processing, the role of array optics is becoming increasingly important as the need for parallelism and density grows for display, communication, and storage applications. This trend toward highly parallel compact optical systems naturally leads to a growing need for high-performance, low-*f*-number ($f^{\#}$) microlens arrays. Refractive microlenses have been used in hybrid optical interconnect strategies,[1–4] switching networks,[5,6] spectrophotometry,[7] confocal microscopy,[8] sensors,[9] focal plane arrays,[10] and photolithography,[9] and applications for such micro-optical elements are only increasing. To address the expanding need for microlenses, fabrication technologies must be identified that will allow lens arrays to be constructed at low cost. In addition, these arrays must be uniform and reproducible so that they can be incorporated seamlessly into existing optical architectures and systems.

Several authors have proposed and demonstrated techniques that enable the fabrication of microlens arrays with the hydrophobic effect.[11–13] We have recently modified these techniques to allow for the assembly of microlenses on hydrophilic domains patterned in an adhesive hydrophobic layer and have characterized the performance of polymer lenses fabricated on a variety of substrates including Si, SiO_2, GaAs, InGaAs, and InP.[14] We demonstrated that these microlenses had low $f^{\#}$s (plano–convex minimum of $f/1.38$), excellent surface profiles (maximum deviation from a sphere was $< \pm 5$ nm over the center 130 μm of 500-μm-diameter $f/3.2$ lenses), and were stable at room temperature for at least 9 months.

Here we report on the optimization of our process to allow for the reproducible fabrication of large, uniform lens arrays. In Section 2 we describe experimental results of lens characterization and optimization. Arrays of microlenses with footprints 2–500 μm in diameter were fabricated by withdrawal of substrates of patterned wettability from a monomer bath at a controlled speed. The fabricated arrays had lithographically defined pitches, allowing for fill factors as great as 90%. At low withdrawal speeds the average $f^{\#}$ of formed lenses could be reduced by means of increasing substrate withdrawal speed or monomer viscosity or decreasing monomer surface tension. At larger withdrawal speeds the average $f^{\#}$ was minimized and became constant, independent of withdrawal speed. This minimum achievable $f^{\#}$ could be reduced by use of a monomer with a large viscosity and large surface tension. At all withdrawal speeds the $f^{\#}$s of formed lenses could

The authors are with the University of California at San Diego, 9500 Gilman Drive, La Jolla, California 92093-0407. D. M. Hartman's e-mail address is hartmann@ece.ucsd.edu.

Received 3 April 2000; revised manuscript received 31 January 2001.

0003-6935/01/162736-11$15.00/0

be reduced by means of decreasing the array fill factor or tilting the substrate so that its patterned side was tilted up during the withdrawal process. Control of the withdrawal speed during fabrication allowed for integration of lenses with different $f^{\#}$s within the same array. The uniformity of lens arrays was analyzed in terms of defect density and lens-to-lens variability. The number of conjoined lenses could be minimized by reduction of the array fill factor, monomer viscosity, and substrate withdrawal speed. In arrays with no defects, an optimum withdrawal speed was shown to exist at which array uniformity was maximized (i.e., the percentage change in the focal length across an array was minimized). At this optimum, arrays of $f/3.48$ microlenses were fabricated by use of one dip-coat with a uniformity of better than $\Delta f/f \sim \pm 3.8\%$. Multiple dip coats allowed for production of arrays of $f/1.38$ lenses with uniformity of better than $\Delta f/f \sim 5.9\%$. Average $f^{\#}$s were reproducible to within 3.5%. These values are competitive with those of leading microlens-fabrication technologies. Finally, other lens characteristics, such as the diameter, shape, and surface roughness of the lenses, were shown to be excellent and independent of the fluid-transfer process.

In Section 3 a model is developed to describe the fluid-transfer process by which monomer solution assembles on the hydrophilic domains, forming lenses under the influence of surface tension. Specifically, equations that describe the fluid-transfer process on homogeneous hydrophilic and hydrophobic substrates are given, and these equations are merged to give an approximate solution for fluid transfer onto a heterogeneously wettable substrate. Although the resulting equations are derived from the analysis of homogeneous substrates, and are therefore inexact for the heterogeneous case, they nonetheless provide insight into the forces governing the lens-forming process. In Section 4 theoretical predictions of lens characteristics are compared with experimental results, and good agreement is found. The conditions that can be used to fabricate optimal lens arrays are stated. Finally, in Section 5, we summarize our results.

2. Experimental Fabrication and Characterization of Microlens Arrays

The method we use to fabricate lens arrays is shown in Fig. 1. An adhesive hydrophobic layer is mechanically applied to the substrate with a polishing cloth. The substrate is then lithographically patterned and the hydrophobic layer selectively etched away from the exposed regions. The substrate is then dipped into and withdrawn from a UV-curable-monomer solution at a controlled speed. As the substrate is withdrawn, the monomer solution drains from the hydrophobic areas of the substrate but remains on the hydrophilic domains. The remaining solution forms spherical caps under the influence of surface tension and can be UV cured to form environmentally stable microlenses.

After curing, if stronger (lower $f^{\#}$) lenses are desired, the substrate may be redipped into the monomer solution. Additional monomer solution assembles on top of the existing cured lenses, causing an increase in the radii of curvature and a corresponding reduction in $f^{\#}$. This process of curing and redipping the substrate may be used repeatedly to reduce the $f^{\#}$s of the fabricated lenses.

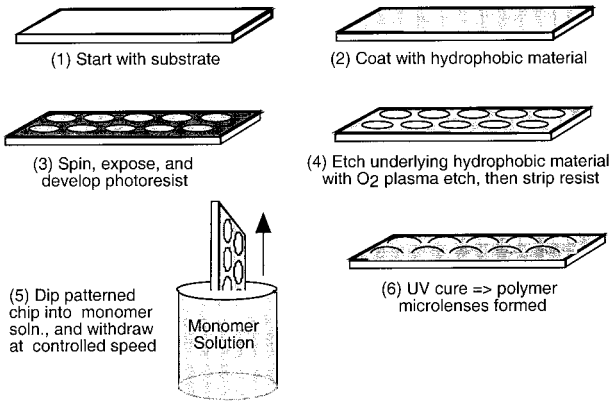

Fig. 1. Process flow for hydrophobic patterning of microlenses.

For consistency we used glass microscope slides as substrates for all experiments conducted here. All monomer solutions used had a density of ~ 1.08 g/cm.[3] Once UV cured, all polymers had an index of refraction of ~ 1.5.

After fabrication, the lenses were characterized. We selected 15–20 lenses across a row of the microlens array under test, and their focal lengths were measured. From these measurements the average $f^{\#}$ and the standard deviation of the focal length for the array were determined. The average $f^{\#}$ was plotted as a function of the variable to be studied, and error bars were included representing one standard deviation from the average value. After completing one set of measurements, the substrate could be redipped into monomer solution, withdrawn at a new speed, and the same lenses could then be measured.

For a given monomer solution, at low withdrawal speeds, increasing substrate withdrawal speed results in a decrease in the $f^{\#}$ of formed lenses. At these speeds, increasing monomer viscosity or decreasing monomer surface tension also results in lower $f^{\#}$s at any given withdrawal speed. These trends can be seen in Fig. 2, which shows average $f^{\#}$ versus withdrawal speed for an array of 500-μm-diameter lenses for two monomer solutions and a $C_3H_5(OH)_3$ (glycerol) solution. The Sartomer CD541 monomer solution has a high viscosity, μ, of ~ 440 centipoise (cP) and a low surface tension, σ, of ~ 35.3 dynes/cm and gives rise to the smallest $f^{\#}$ at all withdrawal speeds shown in Fig. 2. The $C_3H_5(OH)_3$–H_2O solution, with a large viscosity ($\mu \sim 450$ cP) and a large surface tension ($\sigma \sim 64$ dynes/cm) gives rise to slightly larger $f^{\#}$s. Finally, Sartomer SR238 has a low viscosity ($\mu \sim 9$ cP) and a low surface tension ($\sigma \sim 35.7$ dynes/cm) and gives rise to large $f^{\#}$s.

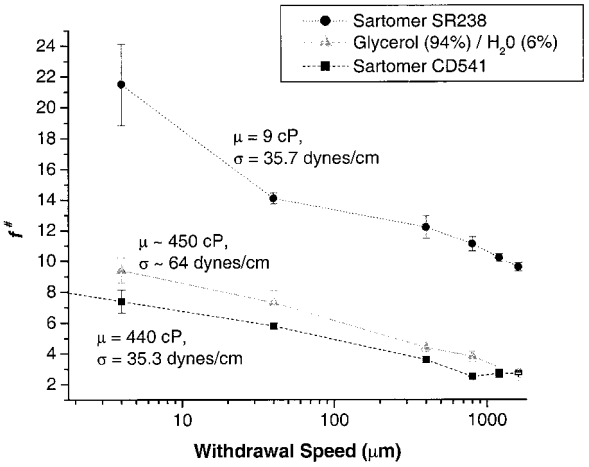

Fig. 2. $f^{\#}$ versus substrate withdrawal speed for 500-μm-diameter lenses (fill factor, ~0.24), for Sartomer CD541 and Sartomer SR238 monomer solutions, and a $C_3H_5(OH)_3$ solution.

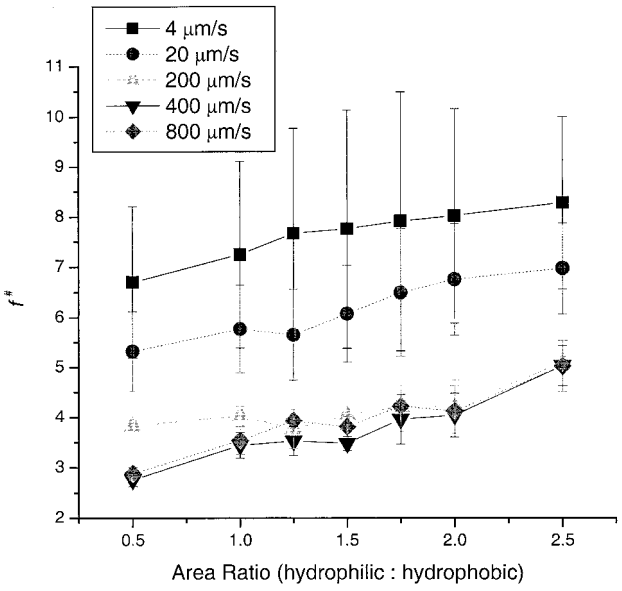

Fig. 3. $f^{\#}$ of 100-μm-diameter lenses made with Sartomer CD541 (μ ~ 440 cP) monomer solution, versus area ratio (hydrophilic area:hydrophobic area) for various withdrawal speeds.

For a given monomer solution, as withdrawal speed is further increased, the $f^{\#}$ reaches a minimum value after which it increases slightly and thereafter remains constant, independent of further increases in withdrawal speed. Figure 2 shows this minimum ($f/\sim 2.5$) for the Sartomer CD541 monomer solution occurring at a withdrawal speed of ~800 μm/s.

Both the minimum value of the $f^{\#}$ that can be achieved and the withdrawal speed at which it occurs are functions of the surface tension and viscosity. Table 1 shows the minimum achievable $f^{\#}$ and the speed at which it occurs for several monomer solutions and a $C_3H_5(OH)_3$–H_2O solution. It can be seen from the table that the smallest minimum $f^{\#}$ can be achieved for solutions with large viscosities and large surface tensions.

For a given monomer solution the average $f^{\#}$ of the formed lenses decreases as the fill factor of the array decreases (i.e., as the ratio of hydrophilic:hydrophobic area decreases). Shown in Fig. 3 is a graph illustrating this trend for an array of 100-μm-diameter circular microlenses, fabricated from the Sartomer CD541 monomer solution at several different substrate withdrawal speeds.

The average $f^{\#}$ of the formed lenses also depends greatly on the shape of the domains. Because of the large number of possible geometric domain shapes, we have not attempted to quantify the differences between various lens shapes (circular, square, elliptical, and so on). Rather, for consistency, we have used circular domains in characterizing the parameters that affect lens formation. For circular domains the domain diameter does *not* significantly influence the achievable lens $f^{\#}$, provided that the array fill factor is maintained constant (although there are minor differences at low withdrawal speeds). Figure 4 illustrates this fact for 100- and 250-μm-diameter lenses, where the average $f^{\#}$ at various withdrawal speeds is plotted as a function of the array fill factor.

The average $f^{\#}$ of the formed lenses is also dependent on the angle with which the substrate is withdrawn from the monomer bath. If the substrate is withdrawn such that its patterned face is tilted up, the $f^{\#}$s of formed lenses is reduced. Conversely, if the patterned face is tilted down, the $f^{\#}$s of formed lenses is increased. For consistency, all substrates

Table 1. Minimum $f^{\#}$ and the Speed at Which the Minimum $f^{\#}$ is Formed for Several Monomer Solutions and a Glycerol Solution[a]

Monomer Name	Viscosity (cP)	Surface Tension (dynes/cm)	Speed at Which Lens Height Is Maximized ($f^{\#}$ is minimized) (μm/s)	Maximum Lens-Sag Height (μm) and Minimum $f^{\#}$
Sartomer SR238	9	35.7	>7500	34/3.8
Sartomer SR492	90	34.0	1420	37/3.4
Sartomer CD541	440	35.3	680	50/2.6
Sartomer SR601	1080	36.6	340	54/2.4
Glycerol/H_2O*[b]	450	~63.4	~4600	61/2.2

[a]500-μm-diameter lenses, array fill factor ~0.25.
[b]A solution of 94% glycerol, 6% H_2O was used. This mixture was chosen because it has a viscosity approximately equal to that of Sartomer CD541.

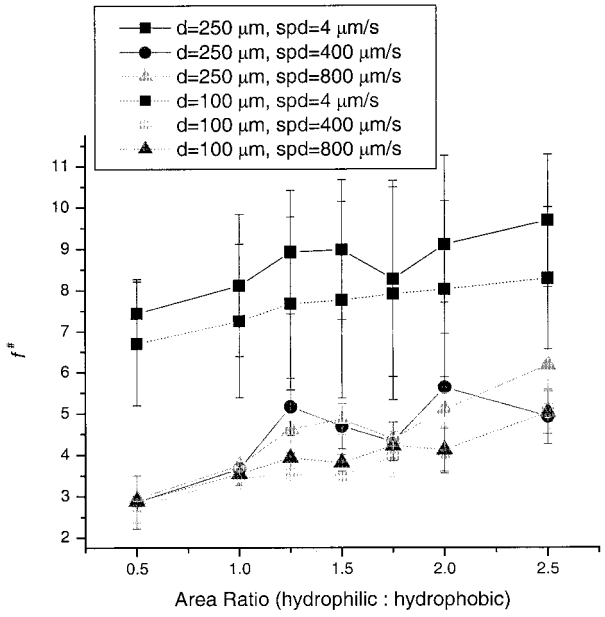

Fig. 4. $f^{\#}$ of 100- and 250-μm-diameter lenses made with Sartomer CD541 (μ ~ 440 cP) monomer solution, versus area ratio (hydrophilic area:hydrophobic area) for various withdrawal speeds.

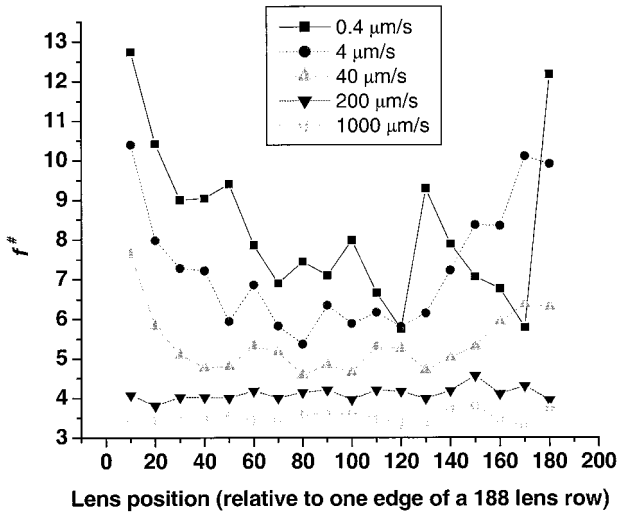

Fig. 5. $f^{\#}$ of 50 μm-diameter microlenses versus the position of the lens in a row of 188 lenses, as measured from one of the edges of the row.

in the experiments we conducted were withdrawn from the monomer solution vertically (with 0-deg tilt).

When all other conditions (i.e., substrate material, withdrawal angle, monomer solution, lens shape and diameter, and array fill factor) are held fixed, the $f^{\#}$ of a fabricated lens depends only on the speed with which the substrate is withdrawn from the monomer solution. When the substrate withdrawal speed is varied *during* the withdrawal process, different $f^{\#}$s can then be integrated in the same array in close proximity. This allows for the implementation of a variety of optical architectures in which it is desired that different rows in an array of microlenses have the same diameters but different $f^{\#}$s.

In addition to the $f^{\#}$ of the lenses, the uniformity of microlenses within an array is a parameter of interest. Analysis of the uniformity of a lens array requires consideration of both the number of defects (lenses that are joined together, missing, or misshapen) within the array and an analysis of the uniformity of those lenses that are not defective.

The number of conjoined lenses within an array is a function of the fill factor of the array, the viscosity of the monomer solution, and the speed with which the substrate is withdrawn. At large fill factors, no conjoined lenses are produced even at high withdrawal speeds. As the fill factor is increased (higher density of lenses), conjoined lenses begin to appear at high withdrawal speeds. If conjoined lenses are produced at a given fill factor, then for a given withdrawal speed more-viscous monomers result in more of these defects than do low-viscosity monomers. Misshapen or missing lenses also occur. These defects can be minimized by use of a monomer with a surface tension that is small enough that the monomer fully wets the hydrophilic areas of the substrate.

Even arrays fabricated with no defects exhibit nonuniformities. These nonuniformities are in the form of lens-to-lens variations in focal length and are a function of the substrate withdrawal speed. At slow withdrawal speeds the $f^{\#}$s of the lenses at the left and the right edges (but not the top and the bottom edges) of an array of lenses are increased to well above the average $f^{\#}$ of lenses in the array. (Here left, right, top, and bottom are defined in relation to how the array is withdrawn from the monomer solution. The top edge of the lens array is the edge that is uncovered first as the substrate is withdrawn.) These edge effects are shown in Fig. 5. At fast withdrawal speeds, nonuniformities also occur. In this case, lenses in the middle of the array have $f^{\#}$s that deviate a great deal from the average value. An optimum withdrawal speed between these two extremes exists at which the uniformity of an array of lenses is maximized. In Fig. 6 the normalized variation in the focal length, $\Delta f/f$, for a row of fifteen 500-μm-diameter lenses (fabricated with a single dip coat) is plotted as a function of the substrate withdrawal speed for two monomer solutions. The more-viscous monomer solution (Sartomer CD541) has a viscosity, μ, of ~440 cP and an optimum withdrawal speed of ~400 μm/s. The medium-viscosity monomer solution (Ciba 5180, μ ~ 200 cP) has an optimum withdrawal speed of ~1200 μm/s. At these optimums, lens arrays made with both these monomers had a uniformity of $\Delta f/f \sim 3.8\%$, corresponding to sag-height variations within the array of $\Delta h/h < \pm 2.5\%$. These values are competitive with leading microlens-fabrication technologies.[15] The uniformity of lens arrays fabricated with multiple dip coats is also improved by means of withdrawing the substrate at an optimum speed. Using the Sartomer CD541 monomer solution and withdrawing the sub-

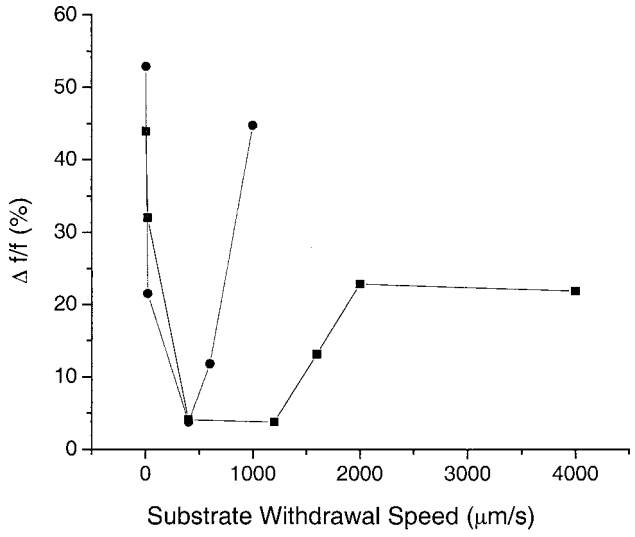

Fig. 6. $\Delta f/f$ versus substrate withdrawal speed for 500-μm-diameter lenses (fill factor, ~0.25), made with Ciba 5180 ($\mu \sim 200$ cP), and Sartomer CD541 ($\mu \sim 440$ cP) monomer solutions.

strate at the optimum withdrawal speed of ~400 μm/s, we fabricated an array of 500-μm-diameter $f/1.38$ lenses, using multiple dip coats with a uniformity of $\Delta f/f \sim \pm 5.9\%$ ($\Delta h/h < \pm 4.5\%$).

The reproducibility of the lens-fabrication process was characterized. Five small-fill-factor (hydrophilic:hydrophobic area ratio of 0.25) lens arrays containing 500-μm-diameter lenses were fabricated with a single 0-deg-tilt dip coat in the high-viscosity monomer (Sartomer CD541, μ~440 cP). The substrates were withdrawn at the optimum withdrawal speed of ~400 μm/s. The average $f^{\#}$ of lenses in these five arrays varied from a minimum of 3.88 to a maximum of 4.02. Thus the average $f^{\#}$ of an array of lenses was reproducible to within (4.02–3.88)/3.95 ~ 3.5%. The apparatus used to withdraw substrates from the monomer solution did not allow for strict control of substrate withdrawal angle; with better control, reproducibility may improve.

In addition to the lens focal length, array uniformity, and reproducibility, there are other lens characteristics that are of interest, including the lens diameter, the lens surface shape (spherical versus aspherical), the roughness of the lens, and the aberrations that result. These characteristics are largely independent of the fluid-transfer process.

The lens diameter is defined only by the size of the hydrophilic domains patterned within the hydrophobic background. The withdrawal speed, tilt angle, array fill factor, monomer viscosity, and monomer surface tension affect the amount of monomer deposited during fabrication, but not the size of the lens footprint. Even multiple dip coats do not affect the lens diameter; additional monomer assembles only on the existing cured lens, a fact that was verified with both optical and atomic force microscopy.

The general shape and surface roughness of lenses formed with our technique are also independent of the fluid-transfer process. As the monomer assembles on the hydrophilic domains, it forms smooth, spherical caps under the influence of surface tension, regardless of the choice of monomer solution, the withdrawal technique, or the number of dip coats used. The caveat is that the lens must remain small (< ~1000 μm in diameter) so that gravity does not influence the shape of the resulting lens. Figure 7 shows optical and atomic force microscope pictures of typical 50-μm-diameter lenses formed with single and multiple dip coats with our fabrication process. It can be seen that the surface profiles of the lenses are quite smooth. Optical profiles (not shown) of such lenses indicate that they deviate from spherical

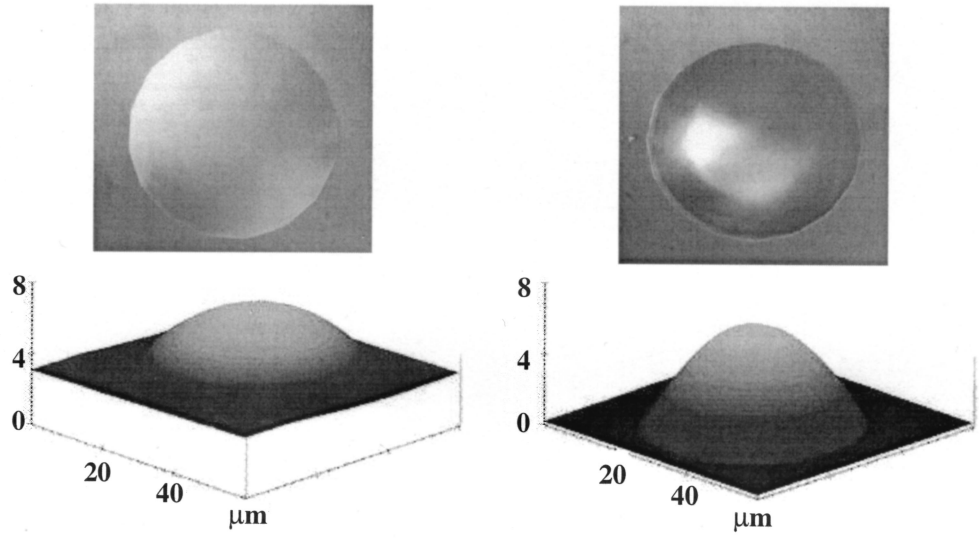

Fig. 7. Optical and atomic force microscope pictures of the surface of a 50-μm-diameter (a) ~$f/3.5$ lens made with one dip coat, (b) ~$f/1.6$ lens made with two dip coats.

by just ± 5 nm for single-dip lenses and by $< \pm 15$ nm for multiple-dip lenses.

Because the lenses formed with this technique have excellent surface profiles, with small deviations from spherical and little surface roughness, aspherical aberrations will be minimized. Also, since most of the potential applications for microlenses involve only on-axis imaging, only spherical and chromatic aberrations will generally be important. Chromatic aberrations can be eliminated through proper selection of a monomer with an index of refraction that is wavelength insensitive over the range of interest. Thus only spherical aberration is of particular concern. Computer simulations, conducted with Code V software (Optical Research Associates, Pasadena, California), were used to determine the point-spread function encircling 84% of the focused energy for various lenses. The point-spread function was shown to range from ~ 8.2 μm for $f/4$ lenses to ~ 47 μm for $f/1.38$ lenses. These values correspond to approximately $2\times$ and $28\times$ the diffraction-limited size of the central Airy disk. If such aberrations cannot be tolerated, input apertures could be fabricated to eliminate nonparaxial rays.

3. Theoretical Modeling of the Lens-Formation Process

A. Background

To understand the trends that have been observed experimentally, it is necessary to consider the process by which fluid is transferred to the hydrophilic domains of a heterogeneously wettable substrate as it is withdrawn from a liquid bath.

Schwartz *et al.* have considered the movement of a liquid layer over a heterogeneous substrate, composed of regular patches of low-energy (hydrophobic) material within a background of high-energy (hydrophilic) material.[16,17] Numerical methods were used to solve the Navier–Stokes equations (momentum conservation for fluids) for the speed $u(x, y, t)$ or the height $h(x, y, t)$ of the liquid layer, at a given location and time on the substrate. The drawback of this approach is that, because there is no analytical solution for these functions, a qualitative assessment of the factors that affect them is not possible. An alternative approach is to consider liquid flow on homogeneous hydrophilic and hydrophobic plates separately and then merge these results to obtain an approximate analytic solution for fluid flow on a heterogeneous substrate. This is the approach we adopt in this paper.

As a clean homogeneous plate is withdrawn from an (uncontaminated) liquid bath, the solid–liquid interaction is characterized by a spreading coefficient, given by Eq. (1)[18]:

$$S_{SL} = \sigma_{SV} - \sigma_{SL} - \sigma_{LV}. \tag{1}$$

Here the σ represent the interfacial free energies per unit area (surface-free energies) of the solid–vapor, solid–liquid, and liquid–vapor interfaces. The liquid–vapor surface-free energy is also referred to as the liquid surface tension. The plate will be wet by the liquid if the spreading coefficient is positive, and for our purposes here this will be considered to be the criterion for a hydrophilic substrate. Conversely, a substrate will be hydrophobic if the spreading coefficient is negative.

The dip coating of a homogeneous hydrophilic substrate, withdrawn vertically from a flat pool of an incompressible Newtonian fluid at a controlled speed, will result in the accumulation of a liquid layer on the hydrophilic surface. The thickness of this film of liquid was first approximated by Landau and Levich[19] and is given by Eq. (2):

$$t = 0.946\,\frac{(\mu U)^{2/3}}{(\rho g)^{1/2}}\left(\frac{1}{\sigma_{LV}}\right)^{1/6} = 0.643\left(\frac{3\mu U}{\sigma_{LV}}\right)^{2/3}(R). \tag{2}$$

Here μ, ρ, and σ_{LV} are the liquid viscosity, density, and surface tension, respectively; g is the acceleration due to gravity; and U is the speed of substrate withdrawal. R is the radius of curvature of the static-meniscus region, which can be shown to be equal to $(\sigma_{LV}/2\rho g)^{1/2}$.[19]

In contrast, a hydrophobic plate withdrawn from a solution will not accumulate a liquid layer on its surface. Rather, the liquid will slip down the substrate. The slip speed, u, between the liquid and the substrate at the liquid–substrate interface is often assumed to be directly proportional to the sheer rate by means of a slip length—that is, $u = \lambda(\partial u/\partial y)$ where λ is the slip length, and y is the distance perpendicular to the substrate surface.[20,21] With this assumption, and with the additional assumptions that the slip speed is small and that the force of gravity is small compared with the liquid surface tension, the maximum speed with which a two-dimensional liquid drop having lateral dimension a_0 will slip down a hydrophobic substrate is given by

$$u = \frac{(a_0\theta_0)^2\,\rho g}{\mu\,\log(2a_0\theta_0/3\lambda)}. \tag{3}$$

Here u is the maximum speed with which the drop slips and should not be confused with the substrate withdrawal speed, U. The density and viscosity of the liquid are represented by ρ and μ, respectively, and g is the acceleration that is due to gravity.[20] The slip length, λ, can be made large when σ_{SL} is made small (i.e., when the substrate is made more hydrophobic).[21,22]

θ_0 is the contact angle of the liquid drop resting on the hydrophobic surface and is given by the following equation:

$$\cos\,\theta_0 = \frac{\sigma_{SV} - \sigma_{SL} + (\tau/r)}{\sigma_{LV}}, \tag{4}$$

where σ_{LV}, σ_{SV}, and σ_{SL} are the surface-free energies (or, equivalently, surface tensions) of the liquid–vapor, substrate–vapor, and substrate–liquid interfaces, respectively. τ is the line tension of the three-phase

contact line, where the solid, liquid, and vapor phases meet, and r is the radius of the base of the drop.[23] In general, for small volumes of liquid, the line tension can have a profound effect on the equilibrium contact angle.[23] However, for the liquid volumes and monomer surface tensions that we used in our experiments, the line tension is small and may be ignored. Equation (4) then reduces to the well-known Young–Dupré equation.[24,25] From this equation it is evident that we can increase the contact angle at the liquid–solid interface by decreasing σ_{SV} (i.e., making the substrate more hydrophobic) or by increasing σ_{LV} (i.e., increasing the liquid–air surface tension).

The speed, u, given by Eq. (3) represents the speed with which an isolated liquid drop, with a constant volume (with lateral dimension a_0), will slip down a uniform hydrophobic substrate. It is not directly applicable to a dip-coating process in which the volume of liquid pulled up from the bath is a dynamic quantity. Nonetheless, Eq. (3) is useful in describing the general trends exhibited in the dip-coating of hydrophobic substrates.

B. Heterogeneous Plate

Liquid draining from the hydrophobic areas of a heterogeneous substrate will follow the same trends as liquid draining from a purely hydrophobic substrate; i.e., the trends will be given by Eq. (3). For instance, an increase in the monomer contact angle or a decrease in monomer viscosity will result in an increased drain speed.

However, on a heterogeneous substrate, hydrophilic domains also exist that will slow the draining liquid as it rolls off the substrate, and the distribution of these hydrophilic domains will affect how the monomer drains. Monomer solution draining from the middle of an array of hydrophilic domains will *feel* more hydrophilic material and drain slower than will monomer solution draining at the left and the right array edges, where a purely hydrophobic environment exists to one side. At the center of the array, where the drain speed reaches a minimum, the drain speed is denoted $U0_{drain}$ and is a function of the amount of hydrophilic material that exists (i.e., the array fill factor). At the left and the right edges of the array the drain speed will attain a maximum value of UE_{drain}. This maximum value of the drain speed is essentially the same as the drain speed of a liquid on a purely hydrophobic substrate and follows the trends of Eq. (3).

Although it is not explicitly indicated, it should be remembered that $U0_{drain}$ is a function of the array fill factor and that both $U0_{drain}$ and UE_{drain} are functions of the monomer viscosity and surface tension [Eqs. (3) and (4)]. Thus the value of $U0_{drain}$ is specific to a given array fill factor, and both $U0_{drain}$ and UE_{drain} are specific to a given monomer solution.

For a given array fill factor and monomer solution, if the substrate is withdrawn at a speed that is less than or equal to $U0_{drain}$, then the withdrawal speed and the drain speed will be one and the same. However, if the substrate withdrawal speed is equal to or greater than the maximum drain speed of the liquid, UE_{drain}, then the liquid will drain at a rate given roughly by Eq. (3), independent of further increases in the substrate withdrawal speed. These two possibilities define two different regimes for the heterogeneous plate, and it is predicted that different trends will be observed in these two regimes.

In the first regime the substrate is withdrawn at a speed that is less than or equal to $U0_{drain}$. The withdrawal speed is therefore the same as the drain speed. In this regime, the amount of liquid that is deposited on the hydrophilic domains will follow the trends given by Eq. (2). Specifically, increasing monomer viscosity or substrate withdrawal speed or decreasing monomer surface tension will give rise to an increase in the sheer force exerted on the monomer solution, which in turn will cause more solution to remain on the substrate.

In the second regime the substrate is withdrawn at a speed that is equal to or greater than UE_{drain}. Increasing the substrate withdrawal speed further will not have an effect on this drain speed—the liquid will drain at a maximum speed, UE_{drain}, given roughly by Eq. (3), regardless of how fast the substrate is withdrawn. The liquid layer thickness that can be deposited at this maximum drain speed can be found by insertion of Eq. (3) into Eq. (2). The following expression results:

$$t \sim \frac{(a_0\theta_0)^{4/3}(\rho g/\sigma)^{1/6}}{[\log(2a_0\theta_0/3\lambda)]^{2/3}}. \tag{5}$$

Here t is the thickness of the liquid adhering to the hydrophilic domains, and all other parameters have been previously defined.

Relation (5) shows that, as expected at the maximum drain speed, the thickness of the liquid layer on the hydrophilic domains is independent of further increases in substrate withdrawal speed. From this equation it can also be observed that, at this maximum drain speed, the liquid layer thickness will no longer be influenced by the liquid viscosity. This can be understood because, as the monomer viscosity increases, the sheer force at any given withdrawal speed increases [Eq. (2)], but the maximum drain speed, UE_{drain}, decreases [Eq. (3)], and these two effects tend to cancel each other. Relation (5) also predicts, however, that the contact angle (partially determined by the surface tension of the monomer) and the slip coefficient (partially determined by the surface tension of the solid–liquid interface) will govern the liquid thickness that can be achieved.

4. Comparison of Theory with Experiment

As predicted by theory, liquid draining from the heterogeneous substrate followed trends given by Eq. (3). Increases in the monomer contact angle (surface tension) and decreases in monomer viscosity resulted in increased drain speeds (Table 1).

The amount of liquid that is deposited on each hydrophilic domain is directly related to the $f^{\#}$ of the resulting lens; more monomer deposition results in a

stronger (lower $f^{\#}$) lens. Thus, in regime 1, in which liquid deposition is governed by Eq. (2), it is predicted that, as the withdrawal speed is increased from zero, the lens $f^{\#}$ will start off large and become progressively smaller as the withdrawal speed is increased up to $U0_{\mathrm{drain}}$. In this regime it is also predicted that, for a given withdrawal speed, monomers with large viscosities and small surface tensions will result in stronger (lower $f^{\#}$) lenses. These are precisely the trends that were observed experimentally in the graph of $f^{\#}$ versus withdrawal speed (Fig. 2).

As the withdrawal speed is increased further, past UE_{drain}, theory predicts the beginning of regime 2. In this regime the lens $f^{\#}$ will be minimized at a constant value, independent of further increases in withdrawal speed [relation (5)]. Relation (5) further predicts that the minimum achievable $f^{\#}$ should be independent of viscosity but highly dependent on monomer surface tension.

Experimentally, it was found that the minimum $f^{\#}$ occurred at a withdrawal speed of $U0_{\mathrm{drain}}$ and increased slightly before becoming constant at higher speeds. This surprising result can be understood because the value of $U0_{\mathrm{drain}}$ is actually a dynamic quantity. If the substrate is withdrawn at a speed of $\leq U0_{\mathrm{drain}}$, the surface tension of the monomer pool exerts a pull on the draining monomer that slightly increases the value of $\mathrm{U0}_{\mathrm{drain}}$. However, if the substrate is withdrawn at a speed of $>\mathrm{U0}_{\mathrm{drain}}$, the draining liquid is further removed from the surface of the monomer pool and the value of $U0_{\mathrm{drain}}$ is reduced. Thus the average $f^{\#}$ of formed lenses is minimized at a withdrawal speed of $\mathrm{U0}_{\mathrm{drain}}$, because this is the fastest speed with which monomer can drain. This was not predicted by theory, because the equations we used were for isolated liquid drops, and the effect of the monomer pool was therefore not considered theoretically. At withdrawal speeds of $>\mathrm{U0}_{\mathrm{drain}}$, however, the $f^{\#}$ of formed lenses does become constant (Fig. 2, Sartomer CD541), in agreement with theoretical predictions.

Experimentally, it was found that the minimum achievable $f^{\#}$ could be made smaller by means of increasing monomer viscosity or surface tension (Table 1). However, from Table 1 it can also be seen that the minimum $f^{\#}$ was far more sensitive to changes in surface tension than to those in viscosity. For instance, the Sartomer SR601 monomer solution has a viscosity that is more than double that of the Sartomer CD541 solution but with approximately the same surface tension. The additional liquid layer thickness deposited by the more-viscous monomer is small (4 μm). However, the $C_3H_5(OH)_3$–water solution has a viscosity similar to that of the Sartomer CD541 solution but with almost double the surface tension. The additional layer thickness deposited by the $C_3H_5(OH)_3$–water solution is large (11 μm). Thus the experimental results differ from theory in that viscosity does affect the minimum achievable $f^{\#}$. However, the relative insensitivity of the minimum $f^{\#}$ to changes in viscosity compared with changes in surface tension is in keeping with theoretical predictions.

Equations (2) and (5) implicitly indicate that the $f^{\#}$s of formed lenses will be a function of the lens array fill factor. This is because, as discussed, arrays with high fill factors will have a smaller $U0_{\mathrm{drain}}$ than arrays with low fill factors. At withdrawal speeds of greater than $U0_{\mathrm{drain}}$ (when arrays of all fill factors are in regime 2) the average $f^{\#}$ of lenses formed on high-fill-factor arrays will therefore become constant at a larger value (the lenses will be weaker) than that of arrays with low fill factors. This trend can be seen in the experimental results of Fig. 3 in which low-fill-factor arrays clearly give rise to lenses with lower $f^{\#}$ at high speeds. However, Fig. 3 also shows that at low withdrawal speeds, $<\mathrm{U0}_{\mathrm{drain}}$, the same trends exist. This is not explained by the model, which predicts that the $f^{\#}$s of lenses formed at speeds of less than $U0_{\mathrm{drain}}$ should be independent of fill factor. The explanation for this discrepancy is that as the monomer solution rolls off the hydrophobic areas of the substrate, it must either drain from the substrate, or snap back onto the hydrophilic domains. Monomer solution draining from arrays with large fill factors does not snap back, but instead drains toward the adjacent (close) row of hydrophilic domains. In contrast, more monomer solution accumulates on the hydrophilic domains of arrays with small fill factors, resulting in stronger (lower $f^{\#}$) lenses even at low withdrawal speeds.

Finally, the $f^{\#}$s of formed lenses will also depend on the substrate dipping angle, because of the effect that the dipping angle has on the shape of the static meniscus. If the substrate is tilted at an angle, the radius of curvature of the static meniscus on the top side of the plate is made larger, whereas the radius of curvature of the static meniscus on the bottom side of the plate becomes smaller.[26] From Eq. (2) it can be seen that these changes in the radius of curvature of the static meniscus will cause a thicker liquid layer to be deposited on the top side while reducing the thickness of the deposited layer on the bottom side. Thus it is expected that, if the patterned side of the substrate is tilted up, stronger (lower $f^{\#}$ lenses) will result. This prediction was confirmed experimentally.

Two factors will influence the achievable uniformity of the lens arrays. First and foremost of these factors is the shape of the three-phase (solid–liquid–air) contact line as it rolls off the substrate. At the left and the right edges of an array of hydrophilic domains there will exist an asymmetrical distribution of hydrophilic area, and the three-phase contact line will be deformed (Fig. 8). More monomer solution will drain from the substrate at these edges, leading to a decrease in liquid volume remaining on the hydrophilic spots and a corresponding increase in the $f^{\#}$ of lenses at the left and the right edges. These predicted edge effects are in accordance with the experimental results of Fig. 5, though it was found that they occurred preferentially at low withdrawal speeds. One possible reason why edge effects tend not to occur at high speeds is that at high speeds the

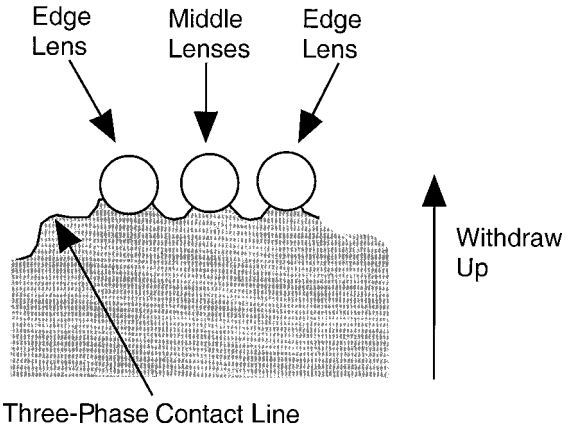

Fig. 8. Schematic of the three-phase contact line as it rolls off the substrate. The contact line is symmetrical in the middle and asymmetrical at the edges.

three-phase contact line does not have time to deform to the extent that it does at low withdrawal speeds.

The shape of the three-phase contact line will also affect the uniformity of the central part of lens arrays (away from the left and the right edges). If the substrate is withdrawn from the monomer solution at a speed no greater than $U0_{\mathrm{drain}}$ (regime 1) a straight solid–liquid–air contact line will be preserved across the entire substrate (except at the edges), and monomer will drain smoothly, generating a uniform lens array. However, if the substrate is withdrawn at a speed greater than $U0_{\mathrm{drain}}$, the three-phase contact line will be deformed, and monomer will drain nonuniformly, leading to nonuniformities in the $f^{\#}$s of the lenses that result.

The second factor that will contribute to array nonuniformity will be that, at low speeds, a relatively small amount of monomer solution will be deposited in each hydrophilic domain. Because the lenses thus formed have a small volume, they will be quite sensitive; small lens-to-lens volume differences will influence their focal length significantly, resulting in a lens array that is more nonuniform than one fabricated at a higher speed.

On the basis of this discussion, the existence of an optimum withdrawal speed at which the standard deviation of the focal length of lenses in an array is minimized is predicted. This optimum was experimentally verified and shown to occur at a withdrawal speed of $U0_{\mathrm{drain}}$. At this speed, the lens volume is maximized, and the monomer drains as smoothly as possible from the substrate.

On the basis of our experiments and our theoretical analysis, we summarize the requirements that allow for the manufacturing of high-performance (i.e., low $f^{\#}$), uniform, and reproducible microlens arrays with the hydrophobic effect:

(1) To produce single-dip low $f^{\#}$ lenses:
   (a) The substrate withdrawal speed should be made equal to $U0_{\mathrm{drain}}$. Increasing the substrate withdrawal speed further will result in a slight increase in $f^{\#}$.
   (b) A large drain speed, $U0_{\mathrm{drain}}$, is desired. To maximize the drain speed:
      (i) A large liquid–solid contact angle is desirable on the hydrophobic regions of the substrate. This can be achieved by means of decreasing the energy of these regions (by use of a more hydrophobic adhesive layer) or increasing the monomer surface tension.
      (ii) A large slip coefficient, λ, is desired. λ can be made large by means of minimizing the substrate–liquid interface energy (by use of a more hydrophobic adhesive layer).
   (c) A viscosity greater than or equal to ~200 cP is desired. Theoretically, at speeds equal to or greater than $U\mathrm{E}_{\mathrm{drain}}$, the layer thickness (and hence the resulting lens $f^{\#}$) should not depend on viscosity. Experiments show, however, that a viscosity of ~200 cP or greater is needed to minimize $f^{\#}$.
(2) To maximize uniformity:
   (a) To prevent severe defects, hydrophilic and hydrophobic regions of the substrate must have positive and negative spreading coefficients, respectively [Eq. (1)].
   (b) The number of conjoined lenses can be reduced by means of reducing the fill factor of the array. If this is not an option, withdrawal speed and/or monomer viscosity must be reduced.
   (c) Assuming a small enough fill factor that conjoined lenses are not generated, substrates should be withdrawn at $U0_{\mathrm{drain}}$, the maximum speed with which liquid can drain from the central portion of the array while still preserving a uniform three-phase contact line.
   (d) Extra dummy lenses should be fabricated to the left and the right sides of an array so that edge effects can be ignored. This is particularly important in high-fill-factor arrays, in which the withdrawal speed must be kept small ($<U0_{\mathrm{drain}}$) to avoid production of defects.
(3) For best reproducibility, careful control of substrate dipping angle is required.

5. Conclusion

In summary, the performance of polymer microlens arrays fabricated by dip-coating patterned hydrophilic:hydrophobic substrates was quantitatively analyzed and optimized. At low withdrawal speeds the average $f^{\#}$ of formed lenses could be reduced by means of increasing substrate withdrawal speed or monomer viscosity or decreasing monomer surface tension. At larger withdrawal speeds, the average $f^{\#}$ was minimized and became constant, independent of withdrawal speed. The minimum $f^{\#}$ was achieved at a withdrawal speed of $U0_{\mathrm{drain}}$, corresponding to the maximum speed with which monomer solution can drain smoothly from the substrate while still preserving a straight liquid–air–solid contact line. The minimum achievable $f^{\#}$ could be reduced by use of a

monomer with a large viscosity and large surface tension. At all withdrawal speeds, the $f^{\#}$s of formed lenses could be reduced by means of decreasing the array fill factor or tilting the substrate so that its patterned side was tilted up during the withdrawal process. Dynamic control of the withdrawal speed allowed lenses with the same diameter but different $f^{\#}$s to be fabricated within the same array. Uniformity of lens arrays was analyzed with an eye to both reducing defect density and minimizing lens-to-lens variations in arrays. We reduced the number of conjoined lenses by making fill factors sufficiently small or by reducing the monomer viscosity or withdrawal speed. We reduced the number of missing and misshapen lenses by ensuring that the monomer surface tension was small enough that the monomer fully wet the hydrophilic domains. In lens arrays in which defects were not a problem, $U0_{\mathrm{drain}}$ was shown to be the optimum withdrawal speed at which array uniformity was maximized. At this optimum, arrays of $f/3.48$ microlenses were fabricated by use of one dip coat with uniformity of better than $\Delta f/f \sim \pm 3.8\%$. Multiple dip coats allowed for production of arrays of $f/1.38$ lenses with uniformity better than $\Delta f/f \sim \pm 5.9\%$. Average $f^{\#}$s were reproducible to within 3.5%. Other lens characteristics such as the diameter, shape, and surface roughness of the lenses were shown to be excellent and independent of the fluid-transfer process. A model was developed to describe the fluid-transfer process by which monomer solution forms lenses on the hydrophilic domains. Good agreement between theory and experimental results was found.

The technique we have developed for the fabrication of microlenses offers several advantages over more conventional methods (resist reflow, ink jet, and others). First, it is extremely low cost, requiring only a mask, and a UV source for the lithographic exposures. Since there is only one masking step, there is no need for an expensive mask aligner. Second, all processing may be performed at room temperature, allowing for integration of lenses with temperature-sensitive materials and components. Third, the polymer lenses are directly fabricated from robust, optically transparent polymers, eliminating the need for an etch transfer step (though such etch transfers may be performed if desired). Finally, our process appears to be competitive with other technologies in offering lithographic alignment, low $f^{\#}$s, large fill factors, spherical surface profiles, and excellent array uniformity and reproducibility. There are, of course, limitations in the technique. For instance, some substrate–liquid systems do not meet the criteria of Eq. (1), and such systems are unsuitable for microlens fabrication. Also, the fabrication of uniform high-fill-factor arrays can be tricky, since it is often necessary to withdraw such substrates below the optimum speed to ensure defect-free arrays. Nonetheless, we feel that for many applications our technique is competitive and in some cases superior to existing microlens-fabrication technologies.

The authors gratefully acknowledge Christoph Berger, Aaron Birkbeck, Cornelius Diamond, Lee Hendrick, Dawei Huang, Philippe Marchand, Mike Sanchez, and Pengyue Wen for discussions and help with optical setups. Jeremy Warner pointed out an important dip-coating paper. Yuri Boiko provided useful advice and help with photopolymerization. Scott Arouh helped in explaining some of the fluid mechanics. Dan Reiley produced optical profiles of the surface of the lenses, allowing surface quality to be assessed. Dan Schickele designed and fabricated one of the substrate withdrawal systems. This research was supported by a grant from the Defense Advanced Research Project Agency, 972–98-1–0001 (Heterogeneous Optoelectronic Technology Center).

References and Note

1. M. R. Taghizadeh, "Micro-optical fabrication technologies for optical interconnection applications," in *Diffractive Optics and Micro-Optics*, Postconference Digest, Vol. 41 of OSA Trends in Optics and Photonics Series (Optical Society of America, Washington, D.C., 2000), p. 260.
2. M. W. Haney, "Micro- versus macro-optics in free-space optical interconnects" in *Diffractive Optics and Micro-Optics*, Postconference Digest, Vol. 41 of OSA Trends in Optics and Photonics Series (Optical Society of America, Washington, D.C., 2000), pp. 266–268.
3. S. Eitel, S. J. Fancey, H. P. Gauggel, K. H. Gulden, W. Bachtold, and M. R. Taghizadeh, "Highly uniform vertical-cavity surface-emitting lasers integrated with microlens arrays," IEEE Photo. Technol. Lett. **12,** 459–461 (2000).
4. G. Sharp and L. E. Schmutz, "Microlens arrays meet any challenge," Lasers Optron. Lasers Optron. **16,** 21–23 (1997).
5. M. C. Wu, L. Y. Lin, S. S. Lee, and C. R. King, "Free-space integrated optics realized by surface-micromachining," Int. J. High Speed Electron. Syst. **8,** 283–297 (1997).
6. M. F. Chang, M. C. Wu, J. J. Yao, and M. E. Motamedi, "Surface micromachined devices for microwave and photonic applications," in *Optoelectronic Materials and Devices*, M. Osinski and Y. Su, eds., Proc. SPIE **3419,** 214–226 (1998).
7. S. Traut and H. P. Herzig, "Holographically recorded gratings on microlenses for a miniaturized spectrometer array," Opt. Eng. **39**, 290–298 (2000).
8. M. Eisner, N. Lindlein, and J. Schwider, "Confocal microscopy with a refractive microlens-pinhole array," Opt. Lett. **23,** 748–749 (1998).
9. P. Nussbaum, R. Volkel, H. P. Herzig, M. Eisner, and S. Haselbeck, "Design, fabrication and testing of microlens arrays for sensors and microsystems," Pure Appl. Opt. **6,** 617–636 (1997).
10. M. E. Motamedi, W. E. Tennant, H. O. Sankur, R. Melendes, N. S. Gluck, S. Park, J. M. Arias, J. Bajaj, J. G. Pasko, W. V. McLevige, M. Zandian, R. L. Hall, and P. D. Richardson, "Micro-optic integration with focal plane arrays," Opt. Eng. **36,** 1374–1381 (1997).
11. E. Kim and G. M. Whitesides, "Use of minimal free energy and self-assembly to form shapes," Chem. Mater. **7,** 1257–1264 (1995).
12. J. L. Wilbur, A. Kurmar, H. Biebuyck, E. Kim, and G. M. Whitesides, "Microcontact printing of self-assembled monolayers: applications in microfabrication," Nanotechnology **7,** 452–457 (1996).
13. H. Biebuyck and G. M. Whitesides, "Self-organization of organic liquids on patterned self-assembled monolayers of alkanethiolates on gold," Langmuir **10,** 2790–2793 (1994).
14. D. M. Hartmann, O. Kibar, and S. C. Esener, "Characteriza-

tion of a polymer microlens fabricated by use the hydrophobic effect," Opt. Lett. **25,** 975–977 (2000).
15. In using the resist reflow process there is a great deal of variability in the sag-height uniformity that can be achieved. Factors that affect the achievable uniformity include the lens pitch, sag height, fill factor, and lens size. Typical sag-height variations range from $44h/h \sim \pm 2$–10%; John Rauseo, MEMS Optical Incorporated, 205 Import Circle, Huntsville Alabama 35806 (personal communication, 2000).
16. L. Schwartz, "Hysteretic effects in droplet motions on heterogeneous substrates: direct numerical simulation," Langmuir **14,** 3440–3453(1998).
17. L. Schwartz and R. Eley, "Simulation of droplet motion on low-energy and heterogeneous surfaces," J. Colloid Interface Sci. **202,** 173–188 (1998).
18. M. Schrader and G. Loeb, eds., *Modern Approaches to Wettability: Theory and Applications* (Plenum, New York, 1992).
19. L. Landau and B. Levich, "Dragging of a liquid by a moving plate," Acta Physicochim. URSS **17,** 43–54 (1942).
20. L. M. Hocking, "Sliding and spreading of thin two-dimensional drops," Q. J. Mech. Appl. Math. **34,** 37–55 (1981).
21. P. Thompson and S. Troian, "A general boundary condition for liquid flow at solid surfaces," Nature (London) **389,** 360–362 (1997).
22. B. Jean-Louis, "Large slip effect at a nonwetting fluid–solid interface," Phys. Rev. Lett. **82,** 4671–4674 (1999).
23. B. Widom, "Line tension and the shape of a sessile drop," J. Phys. Chem. **99,** 2803–2806 (1995).
24. J. Pellicer, J. Manzanares, and S. Mafe, "The physical description of elementary surface phenomena: thermodynamics versus mechanics," Am. J. Phys. **63,** 542–547 (1995).
25. F. Behroozi, H. Macomber, J. Dostal, C. Behroozi, and B. Lambert, "The profile of a dew drop," Am. J. Phys. **64,** 1120–1125 (1996).
26. A. Eberle and A.Reich, "Angle-dependent dip-coating technique (ADDC) an improved method for the production of optical filters. 1. Process flow for hydrophobic patterning of microlenses," J. Non-Cryst. Solids **218,** 156–162 (1997).